Comparison of High Temperature Corrosion Study for FSPed SA-210 Gr A1 and Base Low Carbon Steel

Supreet Singh[a,*], Navneetinder Singh[b], Piyush Bagga[b], Manpreet Kaur[c], Manoj Kumar[1]

[a] *PhD Research Scholar, I.K. Gujral Punjab Technical University, Jalandhar, India*
[b] *M.E. Research Scholar, Deptt. of Automobile Engineering Chandigarh University, Mohali, India*
[c] *Department of Mechanical Engineering, Baba Banda Singh Bahadur Engineering College, Fatehgarh Sahib, India*
[d] *Department of Mechanical Engineering Chandigarh University, Mohali, India*

Abstract

Elevated temperature corrosion is an important material squalor mechanism knowledgeable in boilers in power plants energy generation sectors. Metallic materials such as low carbon steels have special properties such as easy fabrication and machinability, low cost, but a solemn disadvantage of these materials is that the deterioration in properties originating from the interface with the environment and has poor corrosion resistance. The main objective of the current investigation is to achieve strengthening of SA210 Grade A1 boiler steel through microstructural refinement by Friction Stir Processing (FSP) and analyze the effect of the same on high temperature corrosion behaviour. The micro-structural, hardness, tensile and corrosion resistance of the unprocessed and FSPed materials was assessed. The characterization was done by XRD and SEM/EDS analyses with an intend to suggest mechanisms behind high temperature corrosion behavior of the FSPed samples.

Keywords: Friction Stir Processing, Characterization, Corrosion, SEM/EDS/XRD.

1. Introduction

Hot corrosion is identified a serious failure in coal based power plants in India. It has been recognized as an unavoidable and major constraint in the effective operation of boiler of a thermal power plant. Corrosion phenomenon is a most negative parameter and by having an effective control on the formation of rust, the effectiveness of power plant can be improved significantly [1] In the boiler tubes suffering severe fireside corrosion, sulphate salts concentrate at the deposit/scale interface and become partially fused since these salts contain alkali metals of sodium and potassium. The sulphur released from the coal, forms SO_2 with a minor amount of $SO_3$and reacts with the volatilized alkalis to form Na_2SO_4 vapors, which then condense together with fly ash on the pendant superheater and reheater tubes in the boiler [2, 3]. Corrosion control in India is very important in this present time.

Various techniques employed for applying the coatings include, thermal spray, physical and chemical vapor deposition, laser treatment, hard overlays, electroplating and many others. However, various coatings developed using these techniques suffer severe disadvantage such as occurrence of porosity, low adhesion, dilution and non-homogenous microstructure [4–6]. Due to these defects the corrosion-erosion performance of the coatings has been inadequate. Friction Stir Processing is the new and rapid emergent method which is an effective treatment to achieve major microstructural refinement, densification and homogeneity at the processed zone, as well as elimination of imperfections from the manufacturing process. Processed surfaces have shown an improvement of mechanical properties, such as hardness and strength, superior fatigue, enhanced corrosion and wear resistance [7–9].

Figure 1 shows the diagram representation of friction stir processing method. The technique consists of the non-consumable rotating tool carrying a pin and a larger cylindrical body or shoulder which plunges into material until the shoulder presses the substrate surface. The tool thus impels the viscoplastic deformation of its surroundings and, when the proper thermo- mechanical conditions are achieved, the tool initiates its travel movement. Plastic deformation imposed by tool pin and shoulder rotation generates heat which softens the material without reaching its melting point, making it possible to move the pin along the travel direction and the material around the pin [10]. As it travels forward, the workpiece material is moved from the front to the back of the pin, where it is forged under shoulder pressure and merge into a processed bead [11]. As per the survey of the open literature, only limited publications could be found in which wherein FSP of steel has been undertaken. No attempt has been made

*Corresponding Author
Email address: supreet.mech@cumail.com (Supreet Singh)

formerly on FSP of boiler steel with regard to its high temperature corrosion behavior. Materials processed via friction stir processing (FSP) have shown improvement in both hardness and toughness due to microstructural refinement [12–16].

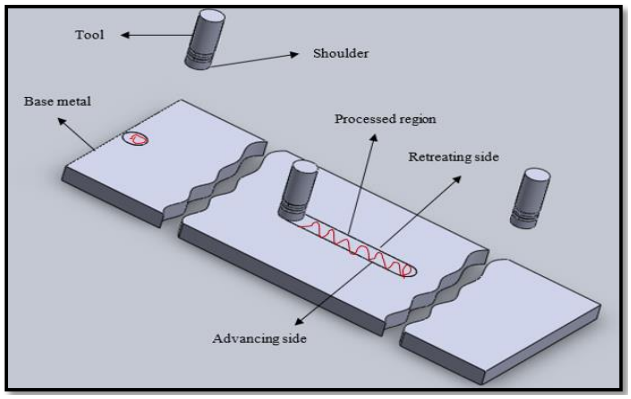

Figure 1: Schematic of Friction Stir Processing

Therefore, the main objective of current investigation is to enhance its surface properties without any pre-treatment. The high temperature corrosion performance of the unprocessed and the FSPed specimens were evaluated in the Na_2SO_4-82% $Fe_2(SO_4)_3$ molten salt environments in the laboratory. The micro-structural, hardness, tensile and corrosion resistance of the unprocessed and FSPed materials were compared. The in-depth characterization was done by XRD and SEM/EDS analyses with an aim to recommend mechanism behind high temperature corrosion behaviour of the FSPed steel.

2. Experimental Procedure

2.1. Friction Stir Processing

The selected steel SA210 Grade A1 (Gr A1) with chemical composition of 0.27 wt.-% C, 0.43 wt.-% Mn 0.21 wt.-%Si 0.035 wt.-%P 0.035 wt.-%S and balance is Fe. The boiler steel plates were cut for FSP conducting tests with defined dimensions 120 mm × 100 mm × 4 mm. FSP was performed on vertical CNC milling machine using a WC tool. The actual FSPed process on Gr A1 steel is shown in Fig. 2. The dimensions of tool are diameter (d) 12 mm and length (l) 90 mm. Friction stir processing was carried using pinless tool with plunge depth of 1 mm, transverse speed as 30 mm per minute and rotational speed of tool as 800 rpm, and 1400 rpm and 2000 rpm with three numbers of passes in each case as defined in Table 1. The samples processed under different rotational speeds were designated as S1, S2 and S3 (here onwards) are shown in Fig. 3. After processing, the test specimens were rapidly cooled using dry ice.

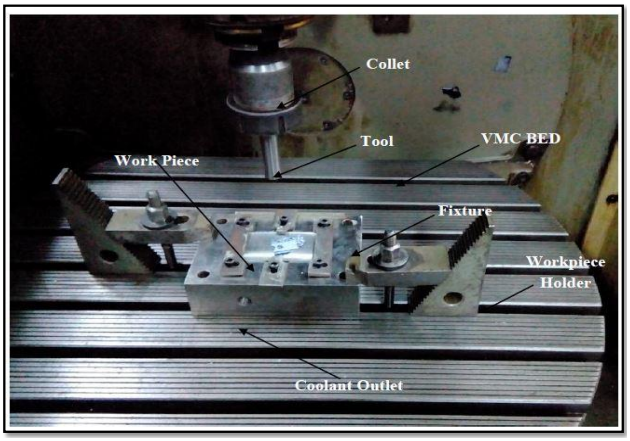

Figure 2: Working set up of Friction Stir Processing on SA 210 Grade A1 steel

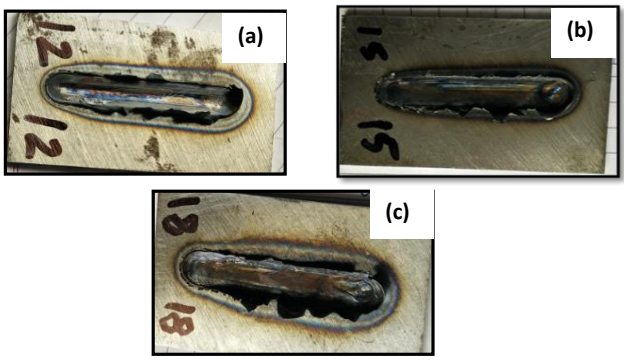

Figure 3: FSP processed Samples (a) S1 (b) S2 and (c) S3

Table 1: Process Parameters of FSP

Sample No.	Process parameters of FSP
S1	800
S2	1400

2.2. Characterizations of Substrate and FSPed Specimens

The FSPed and base material samples were cross-sectioned in a direction perpendicular to stirring zone using low velocity diamond cutter. Thereafter, the hot mountings of cut sections samples in Hydraulic Mounting Press with transoptic powder were done. Samples of boilers steel were polished by means of standard metallurgical course of action to 200 grit size followed by cloth wheel polishing to obtain mirror surface finish. Specimens were then washed with acetone and dried with blower before being examined under the microscope. Optical microscopy built-in with Leica Microsystems software used to examine cross-sectional as well as the surface microstructures of the FSPed specimens and base material. Along with the microstructure of nugget zone, grain size evaluation of the base and FSPed specimens was also observed. The phase transformation study was made using Image processing software "Image-J" at the stirred region of the

specimens of the FSPed specimens.

2.3. High-temperature Corrosion Testing

The specimens each measuring approximately 10 mm × 8 mm × 3 mm was cut into piece as of base and processed steels. High-temperature corrosion studies were done for 50 cycles in the molten salt chemically prepared Na_2SO_4-$82Fe_2(SO_4)$ environments. In the Each cycle one hour of continuous heating at 700°C in a tube furnace followed by twenty (20) minutes of ambient air temperature cooling. The specimens laden boats were set aside inside the tube furnace. The aim of cyclic hot corrosion experimentation is to build up more harsh conditions for testing of specimens than that to face in actual boiler environment. The Na_2SO_4-$82Fe_2(SO_4)$ as a thin layer was coated using a camel brush on the preheated samples (250-300°C) maintaining the uniform thickness of the salt (3 to 5 mg/cm^2). Electronic balance having least count of 1 mg was used to note the change in weight measurements after each cycle. The corroded samples were also integrated in weight measurements to estimate the complete rate of corrosion. The kinetics of the high temperature corrosion was established based on change in weight study after every cycle. The in-depth characterization of corroded samples using SEM/EDS and XRD were also done.

3. Discussion

3.1. Microstructure

The optical microstructures of unprocessed and FSPed steels are shown in Figure 4. The microstructure of the unprocessed steel revealed the presence of ferrite and pearlite (Fig. 4 (a)). The light and dark coloured regions of the microstructure are ferrite and pearlite respectively. The grain boundaries between the grains are clearly visible. The average grain size of the unprocessed steel was found as $25\mu m$. The optical microstructures of the FSPed steel specimens S1, S2 and S3, (Fig. 4 (b), (c) and (d)), illustrates the significant refinement in the microstructure of steel. The average grain size for the S1, S2, and S3 was found to be $4.8\mu m$, $3.22\mu m$ and $2.5\mu m$ respectively. In the nugget zone of S3 specimen had maximum refinement of around 10 folds. According to the studies of Xue *et al.* [17] in case of the microstructural characteristics the grain refinement in the austenitic phase may be attributed to the formation of the martensite formed due to severe plastic deformation. The rapid dry ice cooling rate was sufficient to cause the austenite to martensite phase transformation. The fully dense martensitic microstructure was observed by Image Processing software on Image analyzer. Obviously, the phase transformation occurred during FSP of the Gr A1 steel, indicating that during FSP the temperature was greater than A1, the temperature was greatly reduced due to the rapid dry cooling, and the maximum processing temperature should be lower than Ac3, i.e., within a (γ + α) 2-phase field [18–24]. Therefore, during the processing of Gr A1 steel, part of the novel ferrite phase as well as pearlite altered to the austenite phase, and then transformed into martensite phase during rapid dry ice cooling. Furthermore, dynamic recrystallization of the ferrite and the austenite phases occurred during the FSP process due to the intense plastic deformation, resulting in the ultrafine structure [25–28]. Meanwhile, the original pearlite and ferrite phases were dissolved due to the high temperature and severe plastic deformation during FSP, and diffused into the austensite model. For the FSPed samples, ultrafine dual-phase structure of the ferrite and the martensite phases was achieved in this study.

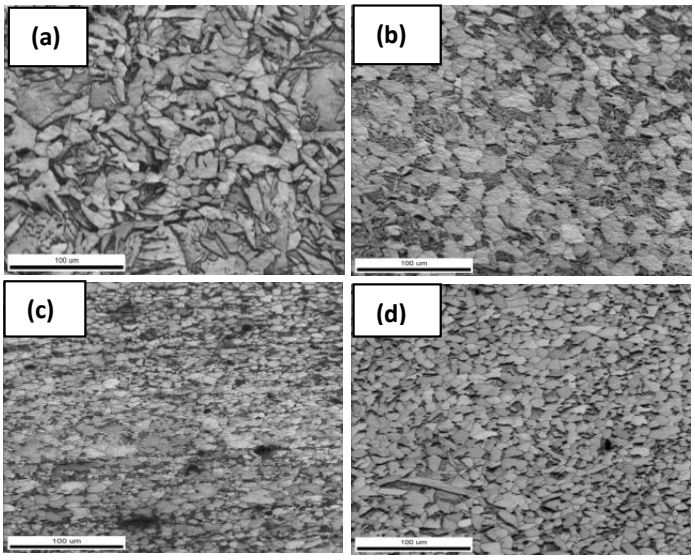

Figure 4: Optical Microscopy showing (a) base steel and FSPed samples at different rpm's (b) S1 (c) S2 and (d) S3.

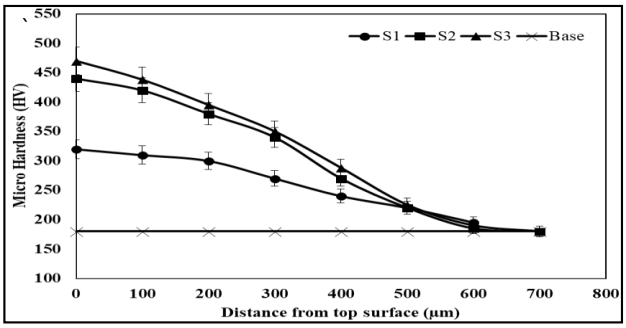

Figure 5: Plot showing the micro-hardness variations along the cross section of the base metal and FSPed SA 210 grade A1 boiler steel.

3.2. Tensile Test

Figure 6 shows the stress-strain curves for the unprocessed and the FSPed specimens. The experimentation showed the higher yield and ultimate

tensile strengths (UTS) of the FSPed specimens and reduced elongations than the unprocessed material. The yield strength (YS) and UTS of the unprocessed steel were about 340 and 470 MPa respectively, and elongation was about 20.3%. After FSP, higher YS of 380 MPa, 410 MPa and 450 MPa was obtained for FSPed specimens S1, S2, and S3 samples respectively. Further, the UTS of 500 MPa, 550 MPa, and 580 MPa was obtained in the processed zone for FSPed specimens S1, S2, and S3 samples respectively. However, the elongation decreased to about 19.02%, 17.1% and 15.2% for the three FSPed specimens respectively. As for the FSPed samples, the increase of the tool rotational speed leads to the increase of the yield and ultimate tensile strength and the small decrease in ductility, consistent with the reduced grain size for the lower heat input condition. In agreement with the hardness observations (5), the improved strength of the FSP samples can be again attributed to the grain structure refinement. In the selected steel, strength and ductility are typically contrasting characteristics. Reduction in grain size decreases the effective distance of slip and accelerates the pile up of dislocations against the grain boundaries i.e. the rate of strain hardening increases. It is believed that the initially higher density of dislocations in the stir zone could assist in increasing the strength and lowering the strain hardening in FSP samples compared with the base metal having coarse grains. In addition, the in homogeneity and instability of plastic deformation in fine grained structures may be another possible cause for the decrease ductility of FSP samples, because the finer the grains are, the lesser the capacity is for a grain to accommodate the dislocations to the increased densities. Hence, the saturation of the dislocation density in the grains of stir zone can also result in the lower strain hardening and decreasing ductility. Compared to the unprocessed steel, high strength was achieved in the FSPed low carbon steels. The highest among all was obtained for S3 specimen. The tensile ductility decreased in the processed steel specimens. Various research studies have also suggested that with the refinement in grains there is increase in strength and reduced ductility [29].However, in FSP samples there is presence of ferrite in martensite which may have resulted in higher hardness and strength but brittle fractured morphology was not complete made on the fracture surface of the FSPed specimens. In the case of base steel the ferrite percentage is greater than martensite due to this ductility was greater and fracture was also brittle [29].

3.3. Visual Observation

Figure 7 (a) shows the hot-corroded unprocessed steel, intensive spallation of the scale was observed from the very first cycle. The spallation continued till the end of the experimentation. Cracks were observed on the surface. The colour of the hot-corroded scale was dark gray with some black spots. On the other hand, the

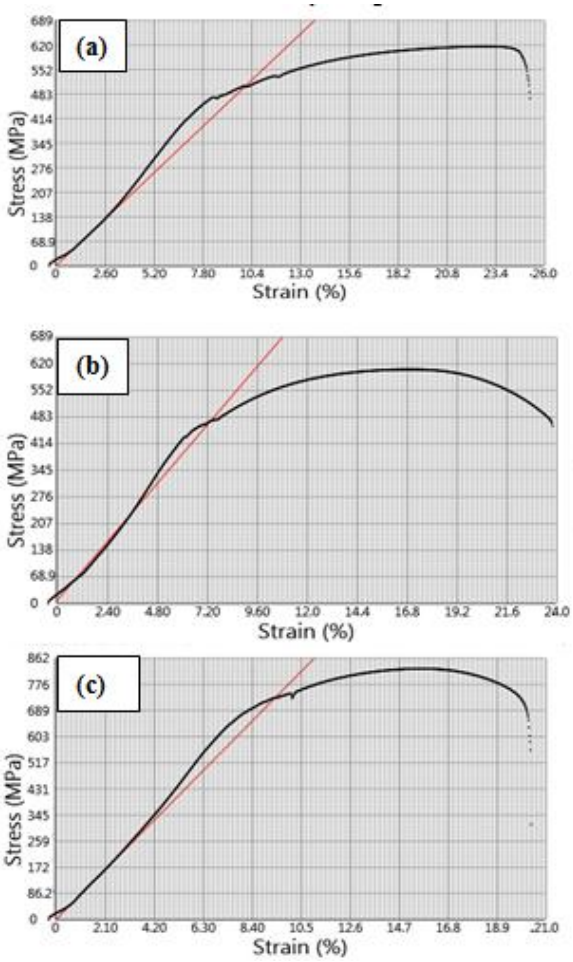

Figure 6: Stress Strain Curve FSPed SA 210 Boiler Steel (a) S1 (b) S2 (c) S3 obtained from tensile test performed at 1x10-3 s-1 strain rate

Table 2: Experimental values of Grain Size, Hardness and tensile properties of the base material and FSP steel

Samples	Average Grain Size	Max. Hardness (Hv)	UTS (MPa)	Elongation (%)
S1	4.8	320	620	25.7
S2	3.2	440	600	23.8
S3	2.5	470	794	20.7

FSPed specimens were initially dark gray in colour. With the increase in the exposure time, some black spots appeared on the lustrous gray scale of S1 specimen shown in Fig. 7 (b). Minor spallation of the hot corroded scale was observed. Scale remained intact without the formation of any cracks till the completion of 50 cycles. In case of S2 Fig. 7 (c) and S3 Fig. 7 (d) specimens, the colour of the scale remained dark gray by the end of the experimentation. No major spallation and cracks were observed during 50 cycles of study in all the FSPed specimens.

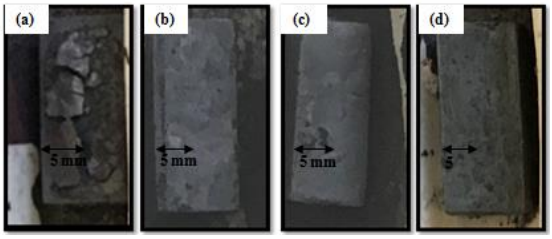

Figure 7: Photographs of a) BM (b) FSPed S1 (c) FSPed S2 (d) FSPed S3 SA 210 Grade A1 boiler steel subjected to cyclic corrosion at 7000C for 50 cycles.

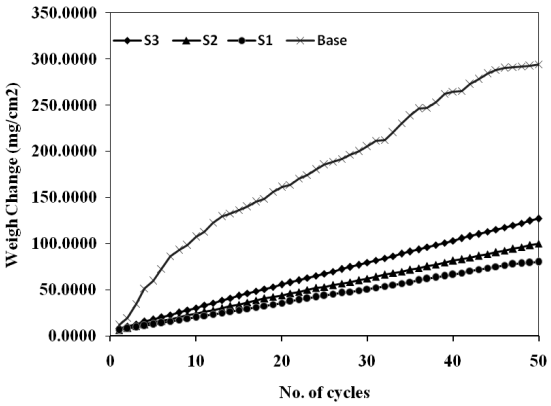

Figure 8: Weight gain vs. number of cycles plots for the unprocessed and FSPed GrA1 steel specimens subjected to Na_2SO_4-82%$Fe_2(SO_4)$ salt environments at 700°C for 50 cycles.

3.4. Weight Change

The weight gain data for the unprocessed and FSPed steel cyclically hot-corroded for 50 cycles at 700°C in Na_2SO_4-82%$Fe_2(SO_4)$ environments is shown in Fig. 8. The plots showed that the unprocessed steel has shown lesser high-temperature corrosion resistance as compared to its FSPed counterparts. During the experimentation, the hot-corroded scale for unprocessed steel showed an intensive tendency towards cracking or spalling. The unprocessed steel showed the overall weight gain of 294.1799 mg/cm^2, which is substantially higher than its FSPed counterparts. The overall weight gain values at the end of 50 cycles for the FSPed S1, S2, and S3 specimens were 79.8942 mg/cm^2, 100.7917 mg/cm^2, and 126.9841 mg/cm^2 respectively. This shows that overall weight gain for the GrA1 steel was decreased by 72.84%, 65.69% and 56.83% which is significant. Therefore, the observations depict that the FSP is positive in enhancing the high-temperature corrosion resistance of the steel. Parabolic rate constant (K_p) values were calculated from the linear regression fitted curves i.e. the parabolic rate constants (K_p) were calculated according to the parabolic rate law of oxidation to establish the rate law for the hot corrosion. The data conforms to the parabolic rate law to an acceptable limit for the FSP at 700°C where $(\Delta W/A) = K_p t$, where $(\Delta W/A)$ is the mass gain per unit area at the oxidation time (t). K_p is equal to the slope of $(\Delta W/A)2$ vs time plot [29]. The unprocessed steel followed the parabolic law of oxidation in general, with some deviations. The Kp value for the unprocessed steel showed transitions $15.3 \times 10^{-10}\, g^2/cm^4/s$ for 50 cycles. The Kp values for FSPed steel S1, S2 and S3 were $4.27 \times 10^{-10}\, g^2/cm^4/s$, $5.72 \times 10^{-10}\, g^2/cm^4/s$, and $6.72 \times 10^{-10}\, g^2/cm^4/s$ respectively.

3.5. XRD/SEM Analysis

The various phases identified from the x-ray diffraction (XRD) patterns of the hot corroded unprocessed and FSPed S1, S2 and S3 specimens in the Na_2SO_4-82%$Fe_2(SO_4)$ molten salt environment at 700 °C for 50 cycles are shown in Fig. 9. The main phases identified for the unprocessed steel were Fe_3O_4(magnetite) as a strong phase and Mn_3O_4 as a medium intensity phase. SiO_2 and $FePO_4$ were observed as the weak intensity phases (Fig. 9 (a)). The performance of various oxides formed on the corroded scale can be explained on the basis of Pilling-Bedworth ratio (P-B ratio RPB) rule. It is the ratio of volume to metal oxide to the volume of corresponding metal. The rule classifies the metals. One that can form protective oxides and the other that cannot. If the ratio is less than unity, the oxide layer is said to be non-protective. It is broken and provides no protecting effect. If the ratio is greater than 2, the scale may chip off and provides no protecting effect. In case the RPB is between 1 and 2, the oxide scale is passivating and provides a protecting effect against further surface oxidation. In case of unprocessed steel, the strong and medium intensity phases possess the RPB greater than 2. The phases provide no protecting effect. Moreover, the scale contained pores and cracks. On the other hand, the scale of the FSPed S1 specimen revealed the presence of Fe_2O_3 and MnO as strong-intensity phases (Fig. 10 (b)). Mn_3O_4 and Fe_2O_3 were observed as the medium-intensity phases. The hot-corroded FSPed S2 specimen was found to have FeO as the strong-intensity phases. MnO were observed as the medium-intensity phases. FeO and Fe_2SiO_4 phase was identified as the weak intensity phase. The hot-corroded FSPed S3 specimen revealed the formation of FeO as the strong-intensity phases with the RPB of 1.92 and 1.75 respectively. Fe_2SiO_4 and FeO and MnO were identified as the medium-intensity phases. Fe_3O_4 phase was identified as the weak intensity phase. The oxides formed are said to be protective. They formed the effective barrier that prevented the metal from internal oxidation. The oxides were passivating and provided a sacrificial effect beside any type of corrosion. The SEM morphology of the unprocessed and FSPed steel specimens subjected to cyclic high-temperature corrosion experimentation in Na_2SO_4-82%$Fe_2(SO_4)$ salt environments is shown in Fig. 10. The oxide scale on the unprocessed steel showed the dominance of Fe with some amounts of C, O, and Mn. The scale revealed the presence of oxides and carbides of

Fe and Mn. The obtained morphology indicates the presence of pores in the hot corroded scale. It is likely that the pores permit the penetration of oxygen inside the unprocessed steel, thus leading to increase in weight.

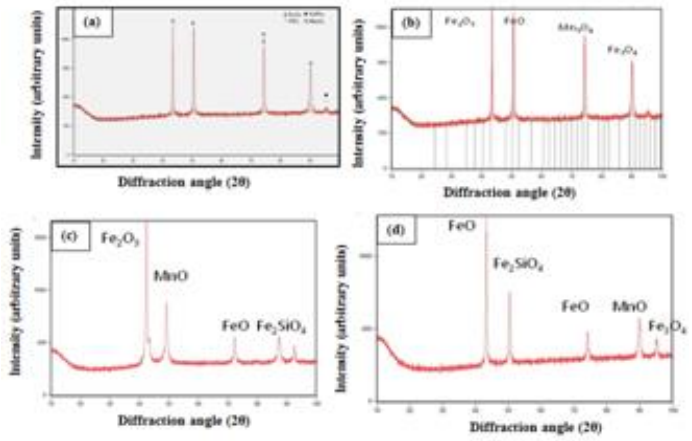

Figure 9: Weight gain vs. number of cycles plots for the unprocessed and FSPed GrA1 steel specimens subjected to Na_2SO_4-82%$Fe_2(SO_4)$ salt environments at 700°C for 50 cycles.

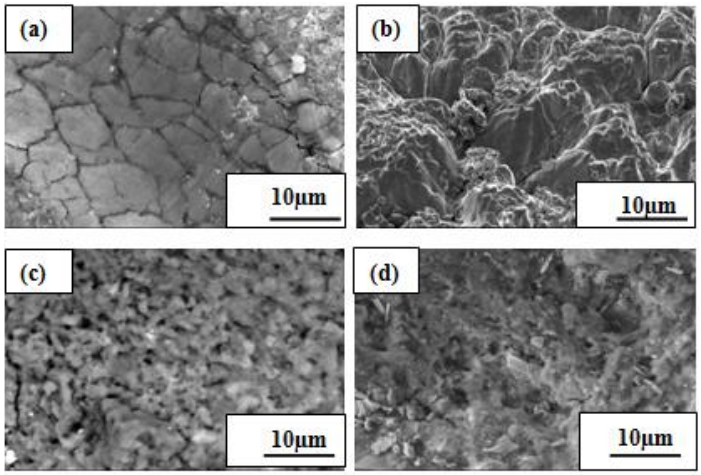

Figure 10: Weight gain vs. number of cycles plots for the unprocessed and FSPed GrA1 steel specimens subjected to Na_2SO_4-82%$Fe_2(SO_4)$ salt environments at 700°C for 50 cycles.

4. Conclusion

1. The transformation of $(\gamma + \alpha)$ 2-phase field to martensite structure by rapid cooling had reduced average grain size to for the S1, S2, and S3 as 4.8 μm, 3.22 μm and 2.5 μm respectively.
2. The FSPed samples showed the enhancement of microhardness by a factor of 1.7, 2.44 and 2.6 times harder for S1, S2 and S3 than that of the unprocessed steel with increasing rotational speed this may be endorsed due to the emergence of fine grain configuration and phase transformation i.e. transformation of austenite to martensite phase and ferrite.
3. FSPed samples, the increase of the tool rotational speed leads to the increase of the yield and ultimate tensile strength and the small decrease in ductility, consistent with the reduced grain size for the lower heat input condition.
4. The high temperature corrosion analyzed the presence of FeO, Fe_2SiO_4, Fe_2O_3 and MnO in the hot-corroded scale of S3 specimen which might have blocked the penetration of oxygen and act as sacrificial oxides .The corroded scale appeared to be very dense in case of FSPed samples with the absence of any pores.

References

[1] http://economictimes.indiatimes.com/opinions/49826868.cms.
[2] G. A.K., M. S, International Journal of Scientific Research (2015) 341–344.
[3] V. Chawla, A. Chawla, D. Puri, S. Prakash, P. G. Gurbuxani, B. S. Sidhu, Hot corrosion & erosion problems in coal based power plants in india and possible solutions–a review, Journal of minerals and materials characterization and Engineering 10 (04) (2011) 367.
[4] F. I. Lathabai S, Ottmuller M, Wear (1998) 93–108.
[5] B. M. Wood R.J.K, Mellor B.G, Wear (1997) 70–83.
[6] H. S. A. Grewal H.S, Arora, Applied Surface Science (2013) 547–555.
[7] E. Nicholas, Friction processing technologies, Welding in the World 47 (11-12) (2003) 2–9.
[8] Thomas, Friction stir but welding 460–317.
[9] B. N. Karthikeyan, Senthilkumar (2009) 2237–42.
[10] L. F. Ma, Z.Y., Mishra (2010) 4693–704.
[11] B. W. Liechty, Journal of Materials Processing Technology (2008) 431–43.
[12] S. M. Anaf E.A, Rayes M.M, Materials and Design (2010) 1231–1236.
[13] F. A. Y. G. M. Z. Ni D.R., Wang D., Scripta Materialia (2009) 568–571.
[14] H. J. Chang C.I, Du X, Scripta Materialia (2008) 356–359.
[15] H. J. Chang C.I, Du X.H, Scripta Materialia (2008) 209–212.
[16] S. C. De P.S., Mishra R.S, Scripta Materialia (2009) 500–503.
[17] P. Xue, W. Li, D. Wang, W. Wang, B. Xiao, Z. Ma, Enhanced mechanical properties of medium carbon steel casting via friction stir processing and subsequent annealing, Materials Science and Engineering: A 670 (2016) 153–158.
[18] H. Bhadeshia, R. Honeycombe, Steels: microstructure and properties, Butterworth-Heinemann, 2017.
[19] Y. H. P.Xue, Z.Y.Ma, Mater (2016) 161–164.
[20] J. C.I. Chang, X.H.Du, Scr.Mater (2007) 209–212.
[21] Z. P.Xue, B.L.Xiao, ActaMetal (2014) 245–251.
[22] C. J.Q. Su, T.W.Nelson, Scr.Mater (2005) 135–140.
[23] Z. P.Xue, B.L.Xiao (2013) 1111–1115.
[24] W. Q. D. W. P.Xue, B.L.Xiao (2013) 30–34.
[25] S.-N. H. S. M.Hajian, Abdollah-zadeh (2014) 184–192.
[26] M. R. A. A.Rahbar-kelishami, A.Abdollah-zadeh (2014) 501–507.
[27] H.-M. Y. H. T.Nagaoka, Y.Kimoto (2015) 224–229.
[28] M. Hajian, A. Abdollah-Zadeh, S. Rezaei-Nejad, H. Assadi, S. Hadavi, K. Chung, M. Shokouhimehr, Microstructure and mechanical properties of friction stir processed aisi 316l stainless steel, Materials & Design 67 (2015) 82–94.
[29] C. Lorenzo-Martin, O. O. Ajayi, Rapid surface hardening and enhanced tribological performance of 4140 steel by friction stir processing, Wear 332 (2015) 962–970.